A semi-Lagrangian deterministic solver for a hybrid quantum-classical nanoMOSFET

Naoufel Ben Abdallah, María José Cáceres, José Antonio Carrillo, Francesco Vecil

SIMAI minisimposia, 15-19/09/2008

Outline

Outline

The model

We afford the simulation of a nanoscaled MOSFET.

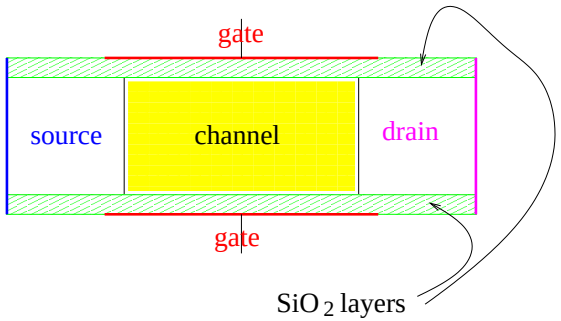

Dimensional coupling

x-dimension is longer than *z*-dimension, therefore we adopt a different description:

- along *x*-dimension electrons behave like particles, their movement being described by the Boltzmann Transport Equation;
- along *z*-dimension electrons confined in a potential well behave like waves, moreover they are supposed to be at equilibrium, therefore their state is given by the stationary-state Schrödinger equation.

The model

Subband decomposition

Electrons in different energy levels, also called *sub-bands*, another name for the eigenvalues of the Schrödinger equation, have to be considered independent populations, so that we have to transport them for separate.

Coupling between dimensions

Dimensions and subbands are coupled in the Poisson equation for the computation of the electrostatic field in the expression of the total density.

Coupling between subbands

Subbands are also coupled in the scattering operator, where the carriers are allowed to jump from an energy level to another one.

The model

Subband decomposition

Electrons in different energy levels, also called *sub-bands*, another name for the eigenvalues of the Schrödinger equation, have to be considered independent populations, so that we have to transport them for separate.

Coupling between dimensions

Dimensions and subbands are coupled in the Poisson equation for the computation of the electrostatic field in the expression of the total density.

Coupling between subbands

Subbands are also coupled in the scattering operator, where the carriers are allowed to jump from an energy level to another one.

The model

Subband decomposition

Electrons in different energy levels, also called *sub-bands*, another name for the eigenvalues of the Schrödinger equation, have to be considered independent populations, so that we have to transport them for separate.

Coupling between dimensions

Dimensions and subbands are coupled in the Poisson equation for the computation of the electrostatic field in the expression of the total density.

Coupling between subbands

Subbands are also coupled in the scattering operator, where the carriers are allowed to jump from an energy level to another one.

Bandstructure

The three valleys

The Si bandstructure presents six minima in the first Brillouin zone:

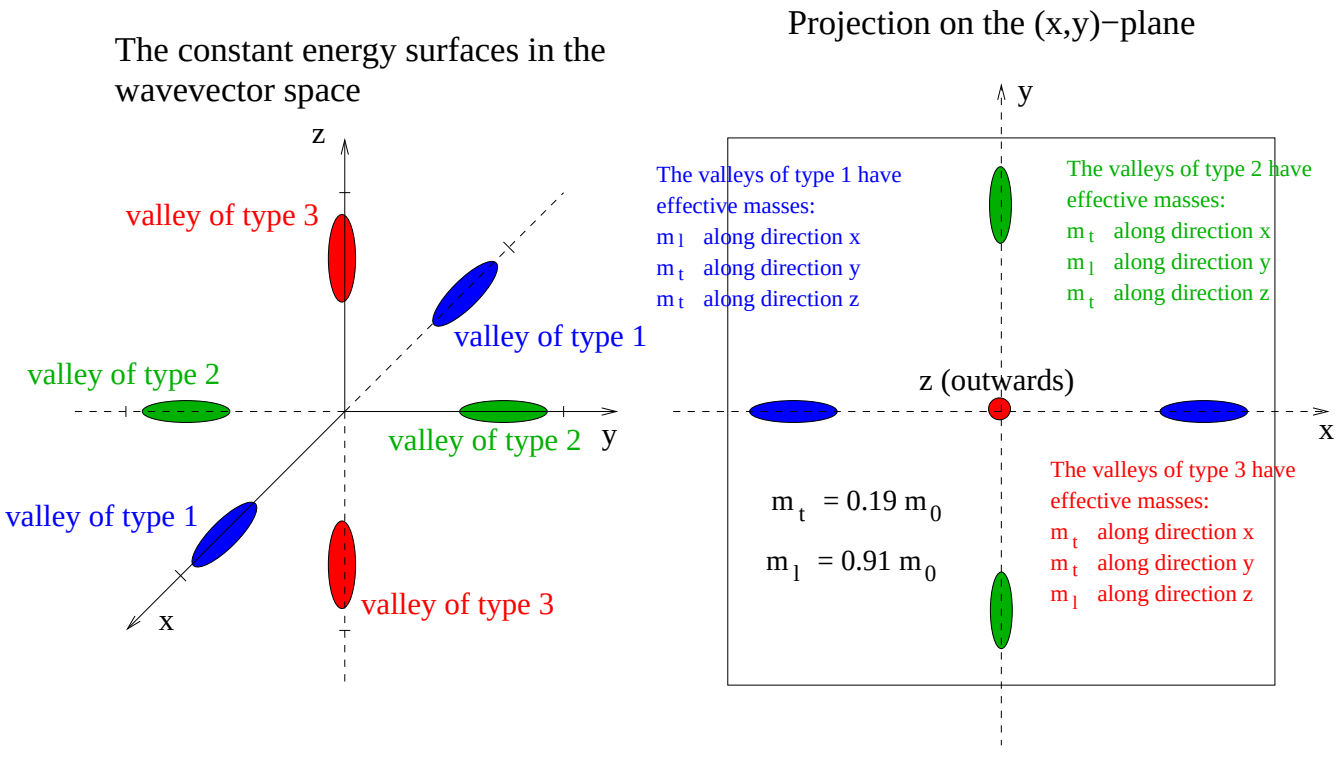

The axes of the ellipsoids are disposed along the *x*, *y* and *z* axes of the reciprocal lattice. The three minima have the same value, therefore there is no gap.

Bandstructure

Non-parabolicity

The bandstructure around the three minima can be expanded following the Kane non-parabolic approximation:

$$\epsilon_\nu^{kin} = \frac{\hbar^2}{1+\sqrt{1+2\tilde{\alpha}_\nu\hbar^2\left(\frac{k_x^2}{m_\nu^x}+\frac{k_y^2}{m_\nu^y}\right)}}\left(\frac{k_x^2}{m_\nu^x}+\frac{k_y^2}{m_\nu^y}\right),$$

where $m_\nu^{\{x,y\}}$ are the axes of the ellispoids (called *effective masses*) of the ν^{th} valley along x and y directions, and the $\tilde{\alpha}_\nu$ are known as Kane dispersion factors.

The simplest case: one-valley, parabolic

$$\epsilon^{kin} = \frac{\hbar^2|k|^2}{2m_*},$$

with m_* an average value between the effective masses.

Bandstructure

Non-parabolicity

The bandstructure around the three minima can be expanded following the Kane non-parabolic approximation:

$$\epsilon_\nu^{kin} = \frac{\hbar^2}{1+\sqrt{1+2\tilde{\alpha}_\nu\hbar^2\left(\frac{k_x^2}{m_\nu^x}+\frac{k_y^2}{m_\nu^y}\right)}}\left(\frac{k_x^2}{m_\nu^x}+\frac{k_y^2}{m_\nu^y}\right),$$

where $m_\nu^{\{x,y\}}$ are the axes of the ellispoids (called *effective masses*) of the ν^{th} valley along x and y directions, and the $\tilde{\alpha}_\nu$ are known as Kane dispersion factors.

The simplest case: one-valley, parabolic

$$\epsilon^{kin} = \frac{\hbar^2|k|^2}{2m_*},$$

with m_* an average value between the effective masses.

Outline

The model

BTE

The Boltzmann Transport Equation (one for each band and for each valley) reads

$$\frac{\partial f_{\nu,p}}{\partial t} + \frac{1}{\hbar}\nabla_k \epsilon_\nu^{kin} \cdot \nabla_x f_{\nu,p} - \frac{1}{\hbar}\nabla_x \epsilon_{\nu,p}^{pot} \cdot \nabla_k f_{\nu,p} = \mathcal{Q}_{\nu,p}[f], \qquad f_{\nu,p}(t=0) = \rho_{\nu,p}^{eq} M.$$

Schrödinger-Poisson block

$$-\frac{\hbar^2}{2}\frac{d}{dz}\left[\frac{1}{m_\nu}\frac{d\chi_{\nu,p}[V]}{dz}\right] - q\left(V + V_c\right)\chi_{\nu,p}[V] = \epsilon_{\nu,p}^{pot}[V]\chi_{\nu,p}[V]$$

$\{\chi_{\nu,p}\}_p \subseteq H_o^1(0, l_z)$ orthonormal basis

$$-\text{div}\left[\varepsilon_R \nabla V\right] = -\frac{q}{\varepsilon_0}\left(\sum_{\nu,p} \rho_{\nu,p}|\chi_{\nu,p}[V]|^2 - N_D\right)$$

plus boundary conditions.

These equations cannot be decoupled because we need the eigenfunctions to compute the potential (in the expression of the total density), and we need the potential to compute the eigenfunctions.

The model

BTE

The Boltzmann Transport Equation (one for each band and for each valley) reads

$$\frac{\partial f_{\nu,p}}{\partial t} + \frac{1}{\hbar}\nabla_k \epsilon_\nu^{kin} \cdot \nabla_x f_{\nu,p} - \frac{1}{\hbar}\nabla_x \epsilon_{\nu,p}^{pot} \cdot \nabla_k f_{\nu,p} = \mathcal{Q}_{\nu,p}[f], \qquad f_{\nu,p}(t=0) = \rho_{\nu,p}^{eq} M.$$

Schrödinger-Poisson block

$$-\frac{\hbar^2}{2}\frac{d}{dz}\left[\frac{1}{m_\nu}\frac{d\chi_{\nu,p}[V]}{dz}\right] - q\left(V + V_c\right)\chi_{\nu,p}[V] = \epsilon_{\nu,p}^{pot}[V]\chi_{\nu,p}[V]$$

$\{\chi_{\nu,p}\}_p \subseteq H_o^1(0, l_z)$ orthonormal basis

$$-\text{div}\left[\varepsilon_R \nabla V\right] = -\frac{q}{\varepsilon_0}\left(\sum_{\nu,p} \rho_{\nu,p}|\chi_{\nu,p}[V]|^2 - N_D\right)$$

plus boundary conditions.

These equations cannot be decoupled because we need the eigenfunctions to compute the potential (in the expression of the total density), and we need the potential to compute the eigenfunctions.

The model

The collision operator

The collision operator takes into account the electron-optical phonon scattering mechanism. It reads

$$\mathcal{Q}_{\nu,p}[f] = \sum_s \sum_{\nu',p'} \int_{\mathbb{R}^2} \left[S^s_{(\nu',p',k')\to(\nu,p,k)} f_{\nu',p'}(k') - S^s_{(\nu,p,k)\to(\nu',p',k')} f_{\nu,p}(k) \right] dk' :$$

every S^s represents a different interaction, which may be elastic or inelastic, intra-valley or inter-valley. Each of them is inter-band.

Structure of the S^s

Each of the S^s consists of a constant, an overlap integral and a delta for the exchange of energy:

$$S^s_{(\nu,p,k)\to(\nu',p',k')} = C_{\nu,\nu'} \int_0^{l_z} |\chi_{\nu,p}|^2 |\chi_{\nu',p'}|^2 dz \delta \left(\epsilon^{tot}_{\nu',p'}(k') - \epsilon^{tot}_{\nu,p}(k) \pm \text{some energy} \right).$$

The model

The collision operator

The collision operator takes into account the electron-optical phonon scattering mechanism. It reads

$$\mathcal{Q}_{\nu,p}[f] = \sum_s \sum_{\nu',p'} \int_{\mathbb{R}^2} \left[S^s_{(\nu',p',k')\to(\nu,p,k)} f_{\nu',p'}(k') - S^s_{(\nu,p,k)\to(\nu',p',k')} f_{\nu,p}(k) \right] dk' :$$

every S^s represents a different interaction, which may be elastic or inelastic, intra-valley or inter-valley. Each of them is inter-band.

Structure of the S^s

Each of the S^s consists of a constant, an overlap integral and a delta for the exchange of energy:

$$S^s_{(\nu,p,k)\to(\nu',p',k')} = C_{\nu,\nu'} \int_0^{l_z} |\chi_{\nu,p}|^2 |\chi_{\nu',p'}|^2 dz \delta \left(\epsilon^{tot}_{\nu',p'}(k') - \epsilon^{tot}_{\nu,p}(k) \pm \text{some energy} \right).$$

Outline

The Newton scheme

The functional

Solving the Schrödinger-Poisson block

$$-\frac{\hbar^2}{2}\frac{d}{dz}\left[\frac{1}{m_\nu}\frac{d\chi_{\nu,p}[V]}{dz}\right] - q\left(V+V_c\right)\chi_{\nu,p}[V] = \epsilon^{pot}_{\nu,p}[V]\chi_{\nu,p}[V]$$

$$-\mathrm{div}\left[\varepsilon_R \nabla V\right] = -\frac{q}{\varepsilon_0}\left(\sum_{\nu,p}\rho_{\nu,p}\left|\chi_{\nu,p}[V]\right|^2 - N_D\right)$$

is equivalt to minimizing, under the constraints of the Schrödinger equation, the functional $P[V]$

$$P[V] = -\mathrm{div}\left(\varepsilon_R \nabla V\right) + \frac{q}{\varepsilon_0}\left(\sum_{\nu,p}\rho_{\nu,p}\left|\chi_{\nu,p}[V]\right|^2 - N_D\right),$$

The scheme

which is achieved by means of a Newton scheme

$$dP(V^{old}, V^{new} - V^{old}) = -P[V^{old}].$$

The Newton scheme

The functional

Solving the Schrödinger-Poisson block

$$-\frac{\hbar^2}{2}\frac{d}{dz}\left[\frac{1}{m_\nu}\frac{d\chi_{\nu,p}[V]}{dz}\right] - q\left(V+V_c\right)\chi_{\nu,p}[V] = \epsilon^{pot}_{\nu,p}[V]\chi_{\nu,p}[V]$$

$$-\mathrm{div}\left[\varepsilon_R \nabla V\right] = -\frac{q}{\varepsilon_0}\left(\sum_{\nu,p}\rho_{\nu,p}\left|\chi_{\nu,p}[V]\right|^2 - N_D\right)$$

is equivalt to minimizing, under the constraints of the Schrödinger equation, the functional $P[V]$

$$P[V] = -\mathrm{div}\left(\varepsilon_R \nabla V\right) + \frac{q}{\varepsilon_0}\left(\sum_{\nu,p}\rho_{\nu,p}\left|\chi_{\nu,p}[V]\right|^2 - N_D\right),$$

The scheme

which is achieved by means of a Newton scheme

$$dP(V^{old}, V^{new} - V^{old}) = -P[V^{old}].$$

The iterations

Derivatives

The Gâteaux-derivatives of the eigenproperties are needed:

$$
\begin{aligned}
d\epsilon_{\nu,p}(V,U) &= -q\int U(\zeta)|\chi_{\nu,p}[V](\zeta)|^2 d\zeta \\
d\chi_{\nu,p}(V,U) &= -q\sum_{p'\neq p}\frac{\int U(\zeta)\chi_{\nu,p}[V](\zeta)\chi_{\nu,p'}[V](\zeta)d\zeta}{\epsilon_{\nu,p}[V]-\epsilon_{\nu,p'}[V]}\chi_{\nu,p'}[V](z).
\end{aligned}
$$

Iterations

After computing the Gâteaux-derivative of the density and developping calculations, we are led to a Poisson-like equation

$$
\begin{aligned}
&-\mathrm{div}\,(\varepsilon_R\nabla V^{new}) + \int_0^{l_z}\mathcal{A}[V^{old}](z,\zeta)V^{new}(\zeta)d\zeta \\
&= -\frac{q}{\varepsilon_0}\left(N[V^{old}]-N_D\right) + \int_0^{l_z}\mathcal{A}[V^{old}](z,\zeta)V^{old}(\zeta)d\zeta,
\end{aligned}
$$

where $\mathcal{A}[V]$ is essentially the Gâteaux-derivative of the functional $P[V]$.

The iterations

Derivatives

The Gâteaux-derivatives of the eigenproperties are needed:

$$
\begin{aligned}
d\epsilon_{\nu,p}(V,U) &= -q\int U(\zeta)|\chi_{\nu,p}[V](\zeta)|^2 d\zeta \\
d\chi_{\nu,p}(V,U) &= -q\sum_{p'\neq p}\frac{\int U(\zeta)\chi_{\nu,p}[V](\zeta)\chi_{\nu,p'}[V](\zeta)d\zeta}{\epsilon_{\nu,p}[V]-\epsilon_{\nu,p'}[V]}\chi_{\nu,p'}[V](z).
\end{aligned}
$$

Iterations

After computing the Gâteaux-derivative of the density and developping calculations, we are led to a Poisson-like equation

$$
\begin{aligned}
&-\mathrm{div}\,(\varepsilon_R\nabla V^{new}) + \int_0^{l_z}\mathcal{A}[V^{old}](z,\zeta)V^{new}(\zeta)d\zeta \\
= &-\frac{q}{\varepsilon_0}\left(N[V^{old}]-N_D\right) + \int_0^{l_z}\mathcal{A}[V^{old}](z,\zeta)V^{old}(\zeta)d\zeta,
\end{aligned}
$$

where $\mathcal{A}[V]$ is essentially the Gâteaux-derivative of the functional $P[V]$.

Outline

Numerical methods

We need to solve the Schrödinger eigenvalue problem and Poisson equations.

The Schrödinger equation

Equation

$$-\frac{\hbar^2}{2}\frac{d}{dz}\left[\frac{1}{m_\nu}\frac{d\chi_{\nu,p}}{dz}\right]-q\left(V+V_c\right)\chi_{\nu,p}=\epsilon_{\nu,p}\chi_{\nu,p}$$

is discretized by alternate finite differences for the derivatives then the symmetric matrix is diagonalized by a LAPACK routine called DSTEQR.

The Poisson equation

We need to solve equations like

$$-\mathrm{div}\left[\varepsilon_R\nabla V\right]+\int_0^{l_z}\mathcal{A}(z,\zeta)V(\zeta)d\zeta=\mathcal{B}(z).$$

The derivatives are discretized by finite differences in alternate directions, the integral is computed via trapezoid rule and the linear system (full) is solved by means of a LAPACK routine called DGESV.

Numerical methods

We need to solve the Schrödinger eigenvalue problem and Poisson equations.

The Schrödinger equation

Equation

$$-\frac{\hbar^2}{2}\frac{d}{dz}\left[\frac{1}{m_\nu}\frac{d\chi_{\nu,p}}{dz}\right]-q\left(V+V_c\right)\chi_{\nu,p}=\epsilon_{\nu,p}\chi_{\nu,p}$$

is discretized by alternate finite differences for the derivatives then the symmetric matrix is diagonalized by a LAPACK routine called DSTEQR.

The Poisson equation

We need to solve equations like

$$-\mathrm{div}\left[\varepsilon_R\nabla V\right]+\int_0^{l_z}\mathcal{A}(z,\zeta)V(\zeta)d\zeta=\mathcal{B}(z).$$

The derivatives are discretized by finite differences in alternate directions, the integral is computed via trapezoid rule and the linear system (full) is solved by means of a LAPACK routine called DGESV.

Numerical methods

We need to solve the Schrödinger eigenvalue problem and Poisson equations.

The Schrödinger equation

Equation

$$-\frac{\hbar^2}{2}\frac{d}{dz}\left[\frac{1}{m_\nu}\frac{d\chi_{\nu,p}}{dz}\right]-q\left(V+V_c\right)\chi_{\nu,p}=\epsilon_{\nu,p}\chi_{\nu,p}$$

is discretized by alternate finite differences for the derivatives then the symmetric matrix is diagonalized by a LAPACK routine called DSTEQR.

The Poisson equation

We need to solve equations like

$$-\mathrm{div}\left[\varepsilon_R\nabla V\right]+\int_0^{l_z}\mathcal{A}(z,\zeta)V(\zeta)d\zeta=\mathcal{B}(z).$$

The derivatives are discretized by finite differences in alternate directions, the integral is computed via trapezoid rule and the linear system (full) is solved by means of a LAPACK routine called DGESV.

Outline

Discretization for the transport

Once we have developped the method for updating the band-potential energies, we can focus the attention on solving the transport. Two discretization are proposed.

Runge-Kutta

FDWENO evaluates via dimension-by-dimension approximation the derivatives $\frac{\partial f_{\nu,p}}{\partial x}$ and $\frac{\partial f_{\nu,p}}{\partial k_1}$ and is coupled with the TVD (Total Variation Diminishing) **Runge-Kutta-3** for the time discretization.

Time- & dimensional-splitting

The BTE is split into the solution of the transport and the collisions, then inside the transport we split dimensions and solve linear advection problems:

$$\begin{aligned} \frac{\partial f_{\nu,p}}{\partial t} + \frac{1}{\hbar}\frac{\partial \epsilon^{kin}_{\nu}}{\partial k_1}\frac{\partial f_{\nu,p}}{\partial x} - \frac{1}{\hbar}\frac{\partial \epsilon^{pot}_{\nu,p}}{\partial x}\frac{\partial f_{\nu,p}}{\partial k_1} &= 0 \\ \frac{\partial f_{\nu,p}}{\partial t} &= \mathcal{Q}_{\nu,p} f\,. \end{aligned}$$

Discretization for the transport

Once we have developped the method for updating the band-potential energies, we can focus the attention on solving the transport. Two discretization are proposed.

Runge-Kutta

FDWENO evaluates via dimension-by-dimension approximation the derivatives $\frac{\partial f_{\nu,p}}{\partial x}$ and $\frac{\partial f_{\nu,p}}{\partial k_1}$ and is coupled with the TVD (Total Variation Diminishing) **Runge-Kutta-3** for the time discretization.

Time- & dimensional-splitting

The BTE is split into the solution of the transport and the collisions, then inside the transport we split dimensions and solve linear advection problems:

$$\begin{aligned} \frac{\partial f_{\nu,p}}{\partial t} + \frac{1}{\hbar}\frac{\partial \epsilon_\nu^{kin}}{\partial k_1}\frac{\partial f_{\nu,p}}{\partial x} - \frac{1}{\hbar}\frac{\partial \epsilon_{\nu,p}^{pot}}{\partial x}\frac{\partial f_{\nu,p}}{\partial k_1} &= 0 \\ \frac{\partial f_{\nu,p}}{\partial t} &= \mathcal{Q}_{\nu,p} f . \end{aligned}$$

Discretization for the transport

Once we have developped the method for updating the band-potential energies, we can focus the attention on solving the transport. Two discretization are proposed.

Runge-Kutta

FDWENO evaluates via dimension-by-dimension approximation the derivatives $\frac{\partial f_{\nu,p}}{\partial x}$ and $\frac{\partial f_{\nu,p}}{\partial k_1}$ and is coupled with the TVD (Total Variation Diminishing) **Runge-Kutta-3** for the time discretization.

Time- & dimensional-splitting

The BTE is split into the solution of the transport and the collisions, then inside the transport we split dimensions and solve linear advection problems:

$$\begin{aligned} \frac{\partial f_{\nu,p}}{\partial t} + \frac{1}{\hbar}\frac{\partial \epsilon_\nu^{kin}}{\partial k_1}\frac{\partial f_{\nu,p}}{\partial x} - \frac{1}{\hbar}\frac{\partial \epsilon_{\nu,p}^{pot}}{\partial x}\frac{\partial f_{\nu,p}}{\partial k_1} &= 0 \\ \frac{\partial f_{\nu,p}}{\partial t} &= \mathcal{Q}_{\nu,p} f. \end{aligned}$$

Runge-Kutta

The operator

Define the operator

$$L_{\nu,p}(t,f) = -\frac{1}{\hbar}\frac{\partial}{\partial k_1}\left[\epsilon^{kin}_{\nu} f_{\nu,p}\right] + \frac{1}{\hbar}\frac{\partial}{\partial x}\left[\epsilon^{pot}_{\nu,p}(t) f_{\nu,p}\right] + \mathcal{Q}_{\nu,p} f,$$

Runge-Kutta scheme

then the third order Total Variation Diminishing Runge-Kutta scheme reads

$$\begin{aligned}
f^{(1)}_{\nu,p} &= f^{n}_{\nu,p} + \Delta t L_{\nu,p}(t^n, f^n) \\
f^{(2)}_{\nu,p} &= \frac{3}{4} f^{n}_{\nu,p} + \frac{1}{4} f^{(1)}_{\nu,p} + \frac{1}{4}\Delta t L_{\nu,p}(t^n + \Delta t, f^{(1)}) \\
f^{n+1}_{\nu,p} &= \frac{1}{3} f^{n}_{\nu,p} + \frac{2}{3} f^{(2)}_{\nu,p} + \frac{2}{3}\Delta t L_{\nu,p}\left(t^n + \frac{\Delta t}{2}, f^{(2)}\right).
\end{aligned}$$

Explicit time-dependence

As a remark, the operator $L_{\nu,p}$ has an explicit time-dependence, because the drain-source potential drop is applied smoothly.

Runge-Kutta

The operator

Define the operator

$$L_{\nu,p}(t,f) = -\frac{1}{\hbar}\frac{\partial}{\partial k_1}\left[\epsilon^{kin}_{\nu} f_{\nu,p}\right] + \frac{1}{\hbar}\frac{\partial}{\partial x}\left[\epsilon^{pot}_{\nu,p}(t) f_{\nu,p}\right] + \mathcal{Q}_{\nu,p} f,$$

Runge-Kutta scheme

then the third order Total Variation Diminishing Runge-Kutta scheme reads

$$\begin{aligned}
f^{(1)}_{\nu,p} &= f^{n}_{\nu,p} + \Delta t L_{\nu,p}(t^n, f^n) \\
f^{(2)}_{\nu,p} &= \frac{3}{4} f^{n}_{\nu,p} + \frac{1}{4} f^{(1)}_{\nu,p} + \frac{1}{4}\Delta t L_{\nu,p}(t^n + \Delta t, f^{(1)}) \\
f^{n+1}_{\nu,p} &= \frac{1}{3} f^{n}_{\nu,p} + \frac{2}{3} f^{(2)}_{\nu,p} + \frac{2}{3}\Delta t L_{\nu,p}\left(t^n + \frac{\Delta t}{2}, f^{(2)}\right).
\end{aligned}$$

Explicit time-dependence

As a remark, the operator $L_{\nu,p}$ has an explicit time-dependence, because the drain-source potential drop is applied smoothly.

Runge-Kutta

The operator

Define the operator

$$L_{\nu,p}(t,f) = -\frac{1}{\hbar}\frac{\partial}{\partial k_1}\left[\epsilon_\nu^{kin} f_{\nu,p}\right] + \frac{1}{\hbar}\frac{\partial}{\partial x}\left[\epsilon_{\nu,p}^{pot}(t) f_{\nu,p}\right] + \mathcal{Q}_{\nu,p} f,$$

Runge-Kutta scheme

then the third order Total Variation Diminishing Runge-Kutta scheme reads

$$\begin{aligned}
f_{\nu,p}^{(1)} &= f_{\nu,p}^{n} + \Delta t L_{\nu,p}(t^n, f^n) \\
f_{\nu,p}^{(2)} &= \frac{3}{4} f_{\nu,p}^{n} + \frac{1}{4} f_{\nu,p}^{(1)} + \frac{1}{4}\Delta t L_{\nu,p}(t^n + \Delta t, f^{(1)}) \\
f_{\nu,p}^{n+1} &= \frac{1}{3} f_{\nu,p}^{n} + \frac{2}{3} f_{\nu,p}^{(2)} + \frac{2}{3}\Delta t L_{\nu,p}\left(t^n + \frac{\Delta t}{2}, f^{(2)}\right).
\end{aligned}$$

Explicit time-dependence

As a remark, the operator $L_{\nu,p}$ has an explicit time-dependence, because the drain-source potential drop is applied smoothly.

Outline

Linear advection

Flux Balance Method:

Total mass conservation is forced. It is based on the idea of following backward the characteristics, but integral values are taken instead of point values:

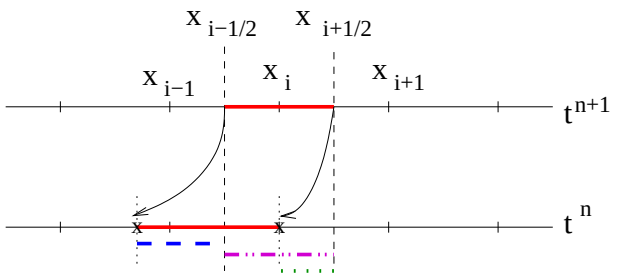

The averages along the red segments are the same, because we have followed the characteristics backward.

FLUX BALANCE METHOD means evualuating the flux at time t^{n+1} from a balance of fluxes at previous time t^n :

- the average along the purple segment
- plus the average along the blue segment
- minus the average along the green segment

Outline

Motivation

We need a **Pointwise** interpolation method which does not add spurious oscillations when high gradients appear, e.g. when a jump has to be transported.

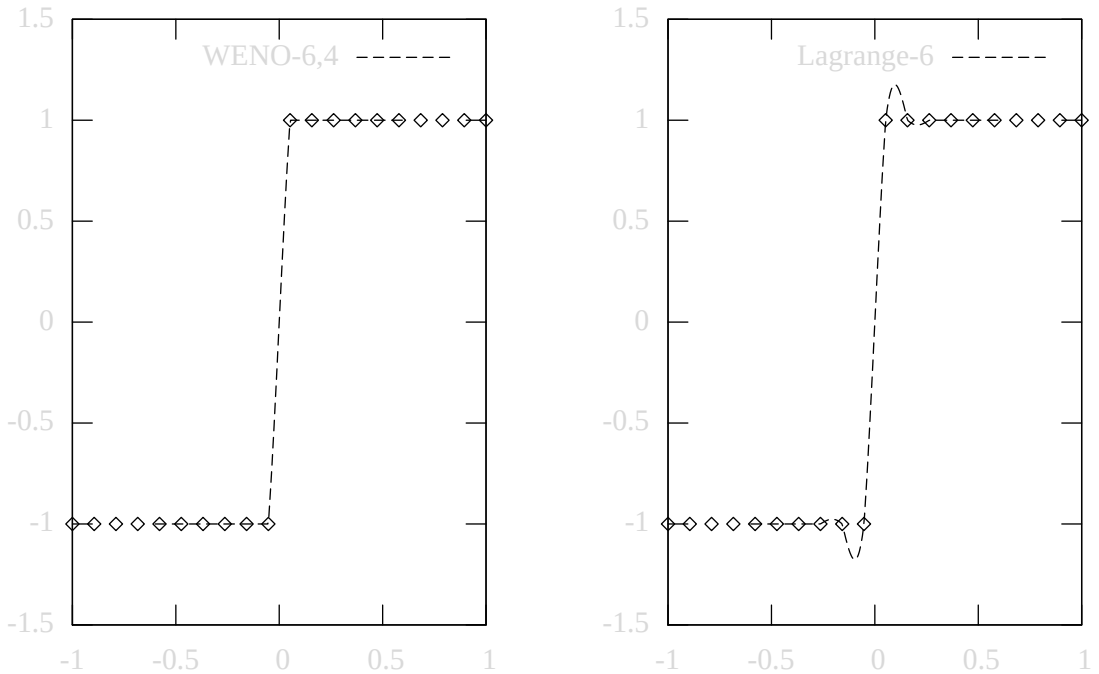

Figure: Left: PWENO interpolation. Right: Lagrange interpolation.

Motivation

We need a **Pointwise** interpolation method which does not add spurious oscillations when high gradients appear, e.g. when a jump has to be transported.

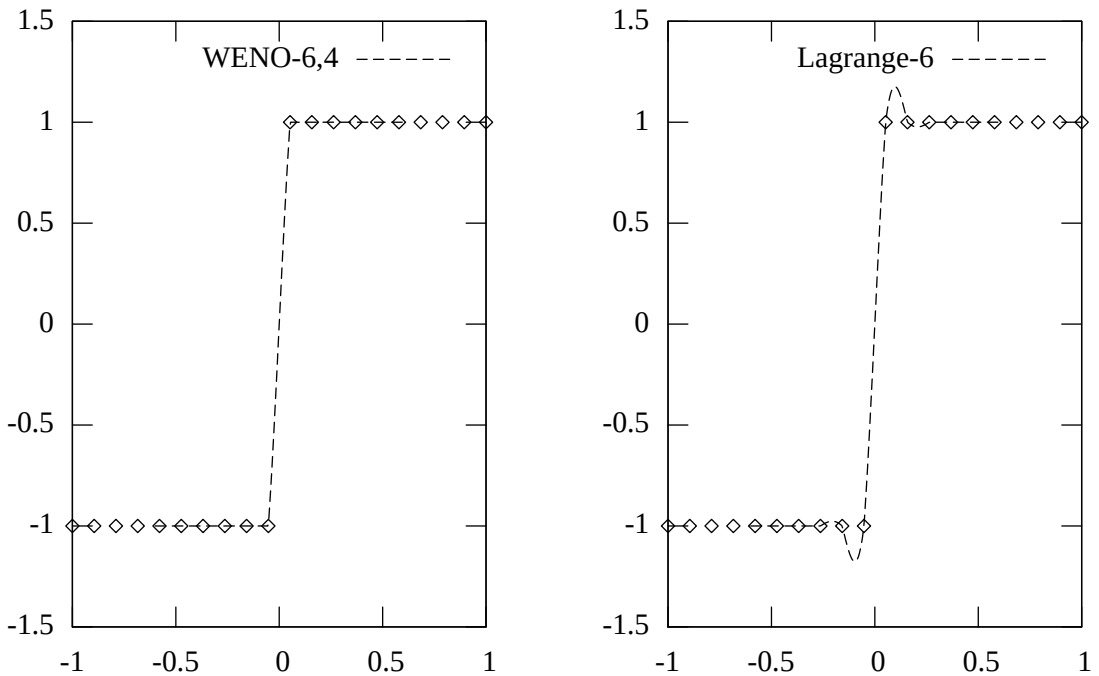

Figure: Left: PWENO interpolation. Right: Lagrange interpolation.

Non-oscillatory properties

Essentially Non Oscillatory (ENO) methods are based on on a sensible average of Lagrange polynomial reconstructions.

We describe the case of PWENO-6,4: we take a stencil of six points and divide it into three substencils of four points:

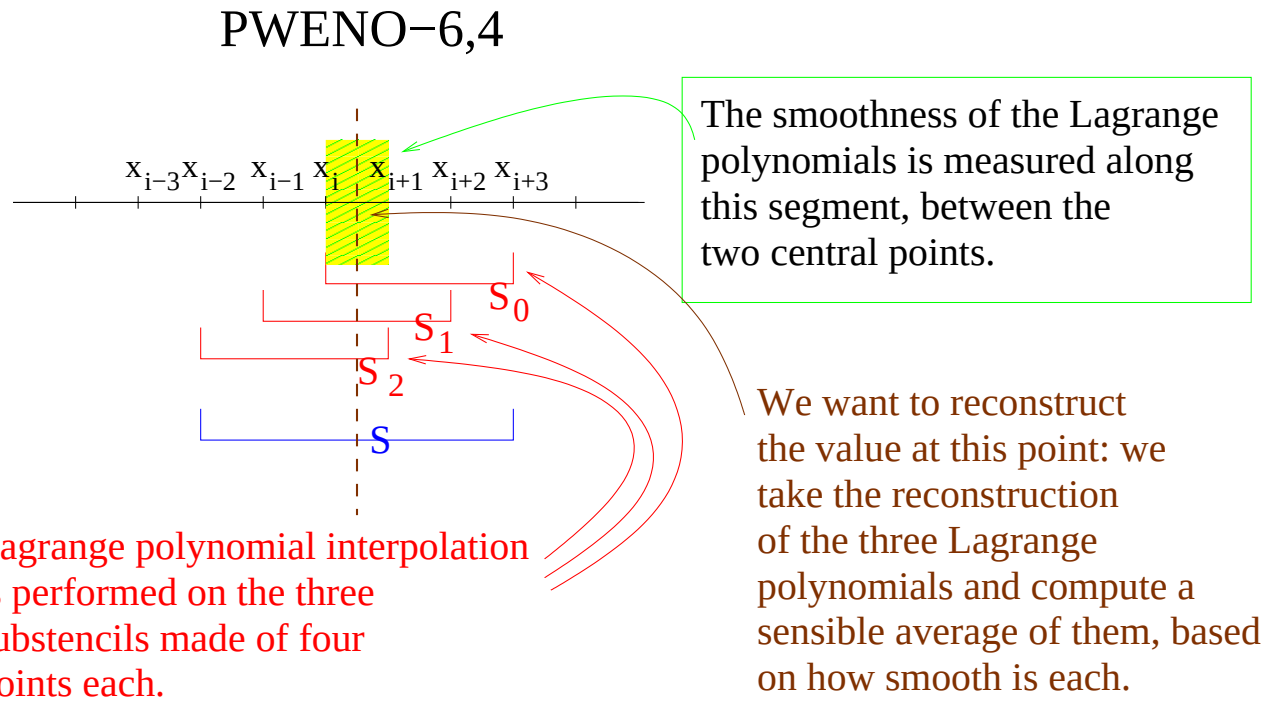

Non-oscillatory properties

Essentially Non Oscillatory (ENO) methods are based on on a sensible average of Lagrange polynomial reconstructions.
We describe the case of PWENO-6,4: we take a stencil of six points and divide it into three substencils of four points:

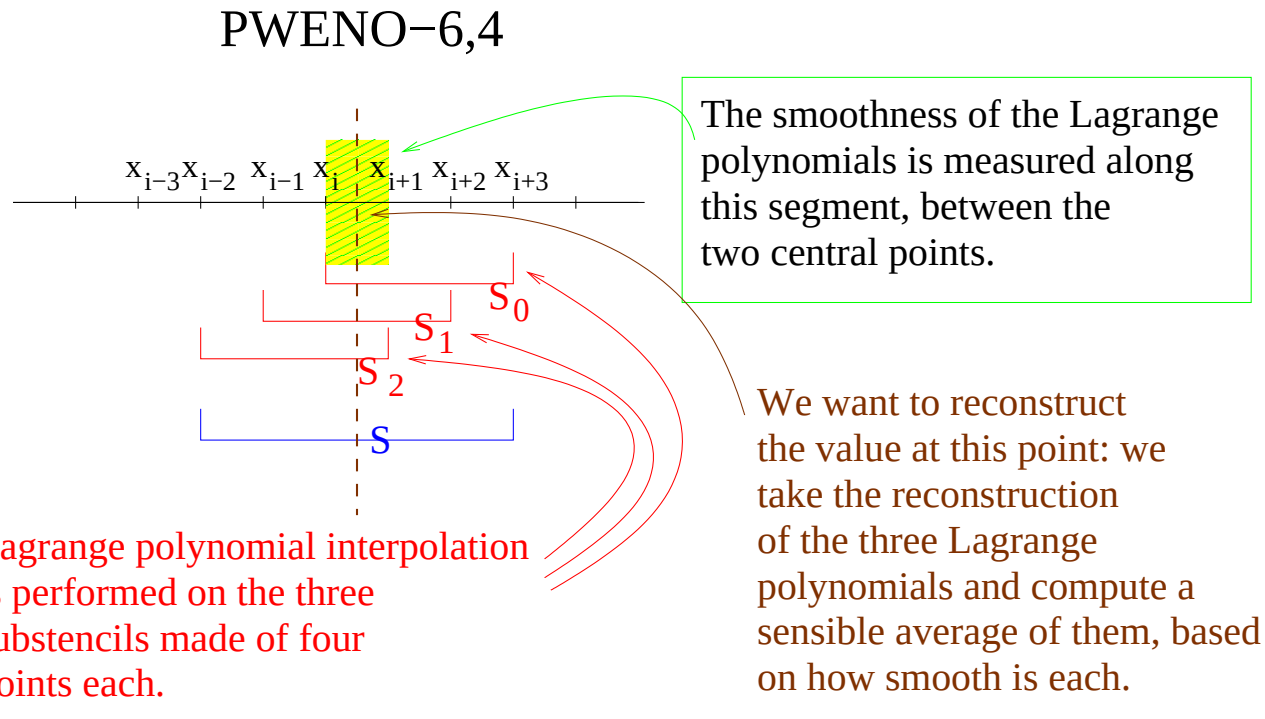

The average

If we note $p_r(x)$ the Lagrange polynomials, PWENO reconstruction reads

$$p_{PWENO}(x) = \omega_0(x)p_0(x) + \omega_1(x)p_1(x) + \omega_2(x)p_2(x).$$

Convex combination.

The convex combination $\{\omega_r(x)\}_r$ must penalize the substencils $\mathcal{S}_r$ in which the $p_r(x)$ have high derivatives.

Smoothness indicators

In order to decide which substencils $\mathcal{S}_r$ are "regular" and which ones are not, we have to introduce the smoothness indicators: we use a weighted sum of the L^2-norms of the Lagrange polynomials $p_r(x)$ to measure their regularity close to the reconstruction point x. The following smoothness indicators have been proposed by Jiang and Shu:

$$\beta_r = \Delta x \left\| \frac{dp_r}{dx} \right\|_{L^2_{(x_i,x_{i+1})}} + \Delta x^3 \left\| \frac{d^2p_r}{dx^2} \right\|_{L^2_{(x_i,x_{i+1})}} + \Delta x^5 \left\| \frac{d^3p_r}{dx^3} \right\|_{L^2_{(x_i,x_{i+1})}}.$$

The average

If we note $p_r(x)$ the Lagrange polynomials, PWENO reconstruction reads

$$p_{PWENO}(x) = \omega_0(x)p_0(x) + \omega_1(x)p_1(x) + \omega_2(x)p_2(x).$$

Convex combination.

The convex combination $\{\omega_r(x)\}_r$ must penalize the substencils $\mathcal{S}_r$ in which the $p_r(x)$ have high derivatives.

Smoothness indicators

In order to decide which substencils $\mathcal{S}_r$ are "regular" and which ones are not, we have to introduce the smoothness indicators: we use a weighted sum of the L^2-norms of the Lagrange polynomials $p_r(x)$ to measure their regularity close to the reconstruction point x. The following smoothness indicators have been proposed by Jiang and Shu:

$$\beta_r = \Delta x \left\| \frac{dp_r}{dx} \right\|_{L^2_{(x_i,x_{i+1})}} + \Delta x^3 \left\| \frac{d^2p_r}{dx^2} \right\|_{L^2_{(x_i,x_{i+1})}} + \Delta x^5 \left\| \frac{d^3p_r}{dx^3} \right\|_{L^2_{(x_i,x_{i+1})}}.$$

The average

If we note $p_r(x)$ the Lagrange polynomials, PWENO reconstruction reads

$$p_{PWENO}(x) = \omega_0(x)p_0(x) + \omega_1(x)p_1(x) + \omega_2(x)p_2(x).$$

Convex combination.

The convex combination $\{\omega_r(x)\}_r$ must penalize the substencils $\mathcal{S}_r$ in which the $p_r(x)$ have high derivatives.

Smoothness indicators

In order to decide which substencils $\mathcal{S}_r$ are "regular" and which ones are not, we have to introduce the smoothness indicators: we use a weighted sum of the L^2-norms of the Lagrange polynomials $p_r(x)$ to measure their regularity close to the reconstruction point x. The following smoothness indicators have been proposed by Jiang and Shu:

$$\beta_r = \Delta x \left\| \frac{dp_r}{dx} \right\|_{L^2_{(x_i,x_{i+1})}} + \Delta x^3 \left\| \frac{d^2p_r}{dx^2} \right\|_{L^2_{(x_i,x_{i+1})}} + \Delta x^5 \left\| \frac{d^3p_r}{dx^3} \right\|_{L^2_{(x_i,x_{i+1})}}.$$

High order reconstruction

Admit for now that the convex combination is given by the normalization $\omega_r(x) = \frac{\tilde{\omega}_r(x)}{\sum_{s=0}^{2} \tilde{\omega}_s(x)}$ of the protoweights $\tilde{\omega}_r(x)$ defined this way:

$$\tilde{\omega}_r(x) = \frac{d_r(x)}{(\epsilon + \beta_r)^2}.$$

Regular reconstruction

Suppose that all the β_r are equal; then we have

$$\omega_r(x) = d_r(x).$$

The optimal order is achieved by Lagrange reconstruction $p_{Lagrange}(x)$ in the whole stencil $\mathcal{S}$, so if we define $d_r(x)$ to be the polynomials such that

$$p_{Lagrange}(x) = d_0(x)p_0(x) + d_1(x)p_1(x) + d_2(x)p_2(x),$$

then we have achieved the optimal order because $p_{PWENO}(x) = p_{Lagrange}(x)$.

High order reconstruction

Admit for now that the convex combination is given by the normalization $\omega_r(x) = \frac{\tilde{\omega}_r(x)}{\sum_{s=0}^{2} \tilde{\omega}_s(x)}$ of the protoweights $\tilde{\omega}_r(x)$ defined this way:

$$\tilde{\omega}_r(x) = \frac{d_r(x)}{(\epsilon + \beta_r)^2}.$$

Regular reconstruction

Suppose that all the β_r are equal; then we have

$$\omega_r(x) = d_r(x).$$

The optimal order is achieved by Lagrange reconstruction $p_{Lagrange}(x)$ in the whole stencil $\mathcal{S}$, so if we define $d_r(x)$ to be the polynomials such that

$$p_{Lagrange}(x) = d_0(x)p_0(x) + d_1(x)p_1(x) + d_2(x)p_2(x),$$

then we have achieved the optimal order because $p_{PWENO}(x) = p_{Lagrange}(x)$.

High order reconstruction

Admit for now that the convex combination is given by the normalization $\omega_r(x) = \frac{\tilde{\omega}_r(x)}{\sum_{s=0}^{2} \tilde{\omega}_s(x)}$ of the protoweights $\tilde{\omega}_r(x)$ defined this way:

$$\tilde{\omega}_r(x) = \frac{d_r(x)}{(\epsilon + \beta_r)^2}.$$

High gradients

Otherwise, suppose for instance that β_0 is high order than the other ones: in this case $\mathcal{S}_0$ is penalized and most of the reconstruction is carried by the other more "regular" substencils.

Outline

Collision operator

Results are presented for the the DG MOSFET in the one-valley, parabolic-band approximation. Moreover, the complete collision operator is substituted by a simple relaxation-time operator:

$$\mathcal{Q}_p f = \frac{1}{\tau} \left(\rho_p M - f_p \right).$$

The goal of this work is just the setting up of numerical tools for a more profound and realistic simulation.
A parallel code in the most realistic case is being implemented.

Outline

Thermodynamical equilibrium: one-valley case

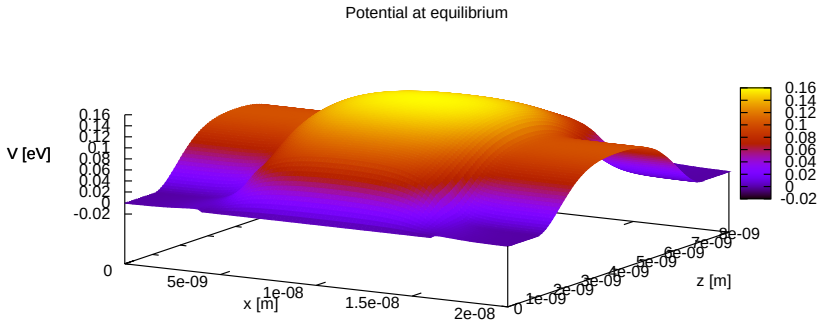

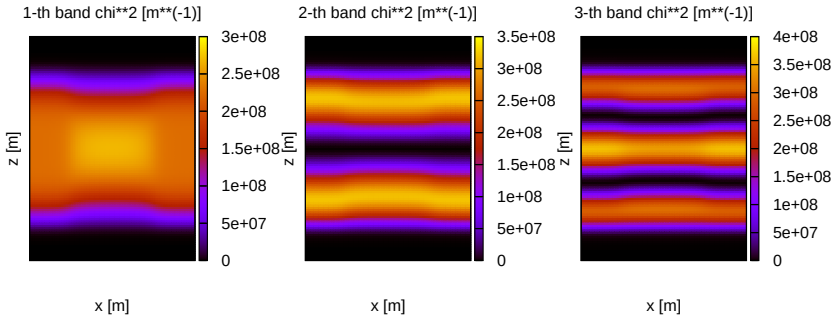

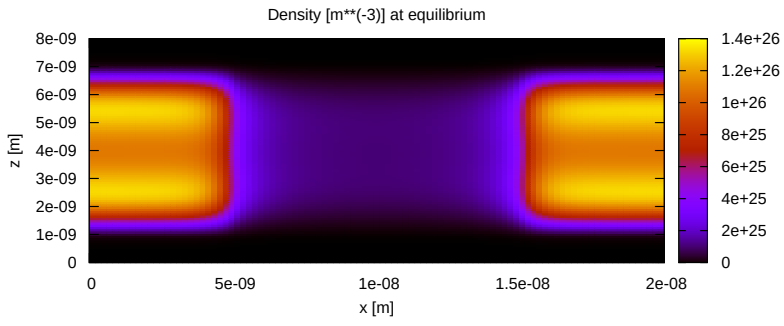

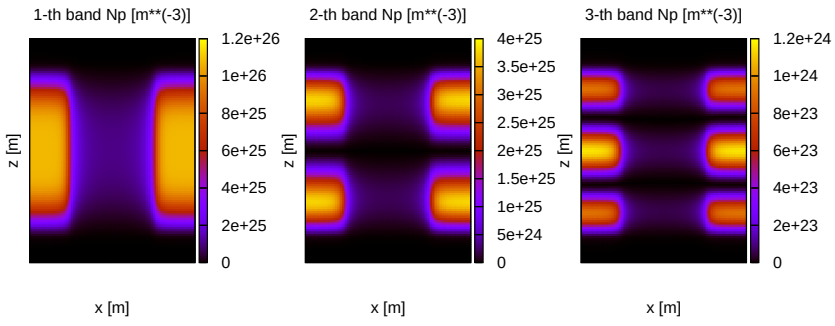

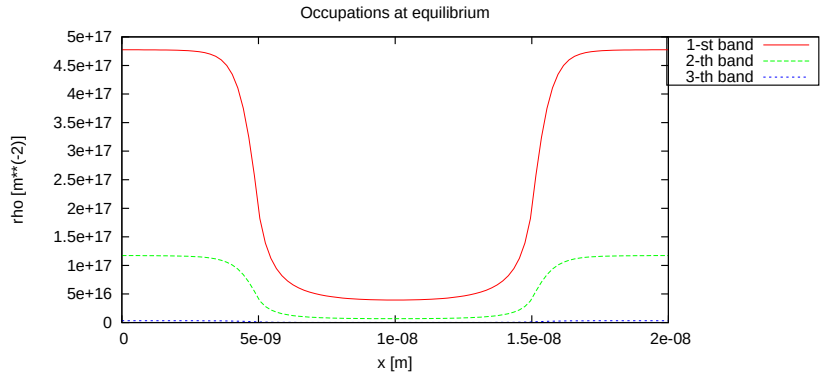

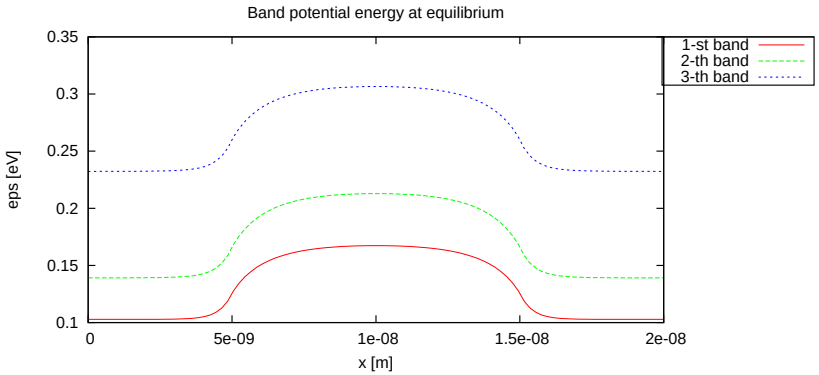

Outline

Long-time behavior

We propose now some results relative to the long-time behavior of the system.